



Published in final edited form as:

*Hepatology*. 2019 July ; 70(1): 84–97. doi:10.1002/hep.30507.

## Deficiency of the mitochondrial glycerol 3-phosphate dehydrogenase contributes to hepatic steatosis

Yi Zheng, Ph.D.<sup>#1</sup>, DR. Hua Qu, M.D., Ph.D.<sup>#1</sup>, Xin Xiong, M.D.<sup>#1</sup>, Yuren Wang, M.D.<sup>#1</sup>, Xiufei Liu, M.D.<sup>#1</sup>, Linlin Zhang, M.D.<sup>1</sup>, Xiaoyu Liao, Ph.D.<sup>1</sup>, Qian Liao, M.D.<sup>1</sup>, Zheng Sun, Ph.D.<sup>2</sup>, Qin Ouyang, Ph.D.<sup>3</sup>, PROF. Gangyi Yang, M.D.<sup>4</sup>, Zhiming Zhu, M.D.<sup>5</sup>, Jing Xu, M.D.<sup>1</sup>, and PROF. Hongting Zheng, M.D., Ph.D.<sup>1,\*</sup>

<sup>1</sup>Department of Endocrinology, Translational Research Key Laboratory for Diabetes, Xinqiao Hospital, Third Military Medical University, Chongqing, China.

<sup>2</sup>Division of Diabetes, Endocrinology and Metabolism, Department of Medicine, Baylor College of Medicine, Houston, Texas, USA.

<sup>3</sup>College of Pharmacy, Third Military Medical University, Chongqing, China.

<sup>4</sup>Department of Endocrinology, the Second Affiliated Hospital, Chongqing Medical University, Chongqing, China.

<sup>5</sup>Department of Hypertension and Endocrinology, Daping Hospital, Third Military Medical University, Chongqing, China.

# These authors contributed equally to this work.

### Abstract

Mitochondrial glycerol 3-phosphate dehydrogenase (mGPDH) is an integral component of the respiratory chain, and recent studies have suggested that it plays an important role in hepatic glucose homeostasis. However, its function in hepatic lipid metabolism is unclear. Here, we identified a role for mGPDH in nonalcoholic fatty liver disease (NAFLD). Specifically, mGPDH expression and activity were lower in fatty livers from NAFLD patients and mice (ob/ob, high-fat diet [HFD] and db/db). Liver-specific depletion of mGPDH in mice or mGPDH knockdown in cultured hepatocytes exacerbated diet-induced triglyceride accumulation and steatosis through enhanced lipogenesis. RNA-seq revealed that mGPDH regulated endoplasmic reticulum (ER)-related proteins and processes. mGPDH deletion exacerbated TM (ER stress inducer)-induced

\* **Correspondence addressed to:** Hongting Zheng, M.D., Ph.D., Department of Endocrinology, Translational Research Key Laboratory for Diabetes, Xinqiao Hospital, Third Military Medical University, Chongqing 400037, China, fnf7703@hotmail.com, Phone: +8602368755709, Fax: +8602368755707. **Reprint requests** Address requests for reprints to: Hongting Zheng, M.D., Ph.D., Department of Endocrinology, Translational Research Key Laboratory for Diabetes, Xinqiao Hospital, Third Military Medical University, Chongqing 400037, China. fnf7703@hotmail.com, fax: +8602368755707.

Author contributions to manuscript

Y.Z., H.Q., X.X., YR.W., XFL. LL.Z. and Q.O.: acquisition of data, analysis and interpretation of data, statistical analysis; Y.Z., H.Q., and X.X.: drafting of the manuscript; X.X., YR.W., XY.L. Q.L. and J.X.: analysis and interpretation of data; Z.S., GY.Y., ZM.Z. and HT.Z.: critical revision of the manuscript for important intellectual content; HT.Z.: study concept and design, analysis and interpretation of data, drafting of the manuscript, critical revision of the manuscript for important intellectual content, obtained study funding, study supervision.

Conflicts of interest

The authors disclose no conflicts.

**Potential conflict of interest:** Nothing to report

hepatic steatosis, while TUDCA (ER stress inhibitor) rescued mGPDH depletion-induced steatosis on a HFD. Moreover, ER stress induced by mGPDH depletion could be abrogated by the intracellular  $\text{Ca}^{2+}$  chelator BAPTA-AM, mitochondrial permeability transition pore (mPTP) inhibitor CsA, or cyclophilin-D (Cyp-D) knockdown. mGPDH promoting Cyp-D ubiquitination was also observed. Finally, liver-specific mGPDH overexpression attenuated hepatic steatosis in ob/ob and HFD mice. **Conclusion:** mGPDH is a pivotal regulator of hepatic lipid metabolism. Its deficiency induces ER stress by suppressing Cyp-D ubiquitination, a key regulator of the mitochondrial  $\text{Ca}^{2+}$  conductance channel mPTP, and results in hepatic steatosis. mGPDH may be a potential therapeutic target for the treatment of NAFLD.

## Keywords

mGPDH; NAFLD; lipogenesis; ER stress

## Introduction

Nonalcoholic fatty liver disease (NAFLD), characterized by excessive hepatic triglyceride (TG) accumulation, is emerging as the most common liver disorder in industrialized countries, and at least 15–30% of people were reported to be affected in a population-based study.<sup>(1)</sup> NAFLD encompasses a pathophysiological spectrum of liver diseases, ranging from simple hepatocellular lipid accumulation (steatosis) to nonalcoholic steatohepatitis (NASH), further progression to cirrhosis, liver carcinoma, and even liver failure and whole body metabolic derangements.<sup>(2)</sup> With its high prevalence and potential for serious sequelae, understanding the mechanisms leading to NAFLD has become a priority.

Mitochondrial glycerol 3-phosphate dehydrogenase (mGPDH, also named *GPD2*), located in the inner mitochondrial membrane, is an integral component of the mammalian respiratory chain. It functions as a rate-limiting step for the glycerophosphate-shuttle by catalyzing the irreversible oxidation of glycerol-3-phosphate (G3P) to dihydroxyacetone phosphate, and concomitantly transfers two electrons from flavin adenine dinucleotide to the electron transport chain.<sup>(3)</sup> Due to differing structures and cell localization, the function and regulation of mGPDH are distinct from those of cytoplasmic glycerol-3-phosphate dehydrogenase (cGPDH, also named *GPD1*).<sup>(4)</sup> mGPDH is abundantly expressed in multiple tissues and organs, and previous studies have demonstrated its pleiotropic effects, such as its participation in thyroid cancer cell growth and metabolism,<sup>(5)</sup> thyroid hormone thermogenesis<sup>(6)</sup> and regulation of sperm capacitation<sup>(7)</sup>. Recently, mGPDH was reported to be involved in hepatic gluconeogenesis,<sup>(8)</sup> but the role of mGPDH in hepatic lipid homeostasis is still unclear. During our study of mGPDH in the context of skeletal muscle regeneration,<sup>(9)</sup> lower mGPDH expression was observed in the livers of ob/ob mice relative to lean mice, which indicated possible relationships for mGPDH with hepatic lipid metabolism and steatosis.

In the present study, we provide in vivo and in vitro evidence to elucidate that the deficiency of hepatic mGPDH seen in both patients and mice with NAFLD contributes to excessive TG accumulation and steatosis by stimulated lipogenesis. RNA-sequencing (RNA-seq) analyses

showed mGPDH was capable of regulating endoplasmic reticulum (ER) homeostasis. mGPDH deficiency caused ER stress by suppressing the ubiquitination of mitochondrial peptidyl-prolylcis-trans isomerase cyclophilin-D (Cyp-D), a regulator of the Ca<sup>2+</sup> conductance channel mitochondrial permeability transition pore (mPTP),<sup>(10)</sup> and resulted in enhanced TG accumulation and steatosis. Moreover, rescue of mGPDH attenuated hepatic steatosis in both HFD- and genetic-induced models, indicating a potential target for NAFLD.

## Materials and Methods

### Animals and treatment

HFD models were established by putting mice on a HFD (fat, 60 Kcal%; protein, 20 Kcal%; carbohydrates, 20 Kcal%; Research Diet, New Brunswick) continuously for the indicated numbers of weeks. To generate liver-specific mGPDH-deficient mice, mGPDH<sup>flox/flox</sup> or mGPDH<sup>flox/wt</sup> mice were transduced with hepatocyte-specific adeno-associated viral 8 (AAV8)-thyroxine-binding globulin (TBG)-cre ( $2 \times 10^{11}$  v.g.), and AAV8-TBG-GFP served as the control.<sup>(11)</sup> To induce acute ER stress, mice were injected intraperitoneally with tunicamycin (TM, Abcam) at 1 mg/kg body weight. To inhibit ER stress, mice were injected intraperitoneally with TUDCA (Sigma-Aldrich) at 500 mg/kg body weight per day. Liver-targeted gene vector AAV8 was used<sup>(12)</sup> for mGPDH overexpression, and the recombinant mGPDH-encoding AAV8 and control vectors (AAV8-GFP) were generated by GENE Company. AAV8-mGPDH ( $2 \times 10^{11}$  v.g.) was injected into mice via the tail vein. For the Cyp-D knockdown experiment, mGPDH liver-specific knockout mice fed HFD for 4 weeks were injected with AAV8-Sh-Cyp-D ( $2 \times 10^{11}$  v.g.), followed by HFD for another 4 weeks. All mice were housed with a standard 12-h dark/light cycle with food and water *ad libitum*. After animals were sacrificed, tissues were immediately snap-frozen and stored at  $-80^{\circ}\text{C}$ , or formalin-fixed for subsequent analysis. All mouse experiments were performed in accordance with protocols approved by the Laboratory Animal Welfare and Ethics Committee of the Third Military Medical University.

In detail, to assess the effects of mGPDH deficiency under normal chow conditions, mGPDH<sup>flox/flox</sup> mice fed with standard chow were injected with AAV8-TBG-cre at 4 weeks of life and sacrificed at 9 weeks of life. To observe the effects of mGPDH deficiency under HFD challenge, mGPDH<sup>flox/flox</sup> or mGPDH<sup>flox/wt</sup> mice fed with standard chow were injected with AAV8-TBG-cre at 4 weeks of life. Two weeks later, mice were switched to the HFD and sustained for 12 weeks. For the TM experiment, mGPDH<sup>flox/flox</sup> mice fed with standard chow were injected with AAV8-TBG-cre at 4 weeks of life. Five weeks later, mice were treated with TM and sacrificed 48 h later. For the TUDCA experiment, mGPDH<sup>flox/flox</sup> mice fed with standard chow were injected with AAV8-TBG-cre at 4 weeks of life. Two weeks later, mice were switched to the HFD for 8 weeks and treated with TUDCA during the last 2 weeks. To evaluate the effects of mGPDH rescue, 8-week-old ob/ob mice were injected with AAV8-mGPDH and sacrificed 8 weeks later. To obtain similar observations in HFD mice, C57BL/6J mice were switched to the HFD at 5 weeks of life. Four weeks later, mice were injected with AAV8-mGPDH. Eight weeks after AAV injection, mice were sacrificed.

### Quantitative real-time PCR (qRT-PCR)

qRT-PCR were performed according to our previous protocol.<sup>(13)</sup> Briefly, total mRNA was isolated from cultured cells or tissue samples using Trizol (Takara), according to the manufacturer's instructions. RNA quality was assessed on a Nanodrop2000 to obtain the 260/280 ratio. Samples with a ratio of 1.8 to 2.0 were processed for gene analysis. One microgram of mRNA was reverse-transcribed into cDNA by using the PrimeScript RT Reagent Kit with gDNA Eraser (Takara) according to the manufacturer's protocol. SYBR Green (Takara) was applied to quantify PCR amplification. Expression levels were calculated using the Ct-method. The primer pairs used in this study are described in Supporting Table S1.

### Lipogenesis assay

Hepatocytes were incubated with 0.2  $\mu\text{Ci/mL}$   $^{14}\text{C}$ -acetate for 2 h, then lysed in NaOH (2.5M) and resuspended in MicroScint-E (PerkinElmer). Radioactivity was quantitatively measured using a Tri-Carb 2910 TR (PerkinElmer).

### Statistical analyses

All data were analyzed using GraphPad Prism 7 (Macintosh). Quantitative values are presented as the mean  $\pm$  S.E.M. Statistical differences between two experimental groups were analyzed by 2-tailed Student's *t*-test. For multiple comparison analysis, one-way ANOVA followed by Tukey's multiple comparison tests were performed.

## Results

### mGPDH expression and activity are downregulated in the livers of NAFLD patients and mice

To investigate the possible association between mGPDH and liver lipid metabolism, we first observed hepatic mGPDH expression in NAFLD mice models (*ob/ob*, HFD and *db/db*). Both mGPDH mRNA and protein levels were decreased in the livers of all three models relative to the corresponding control (normalized to both GAPDH and a mitochondrial protein OTC) and showed an inverse correlation to the induction of fatty acid synthase (FASN), an indicator of liver steatosis (Fig. 1A,B). A reduction in mGPDH activity and increase in the concentration of G3P (substrate of mGPDH) were also observed (Fig. 1C,D). Moreover, in the livers of NAFLD patients, mRNA and protein levels of mGPDH were reduced (ChiCTR-ROC-17010719, Fig. 1E-G), which was consistent with the observations obtained from mouse models. The simultaneous downregulation of mGPDH expression and activity observed in NAFLD patients and mice indicates the potential involvement of mGPDH in hepatic lipid metabolism and steatosis.

### Hepatic mGPDH deficiency exacerbates TG accumulation and steatosis

To explore the impact of downregulated mGPDH on hepatic lipid metabolism, hepatocyte-specific mGPDH-deficient mice generated by mGPDH<sup>flox/flox</sup> transduced with AAV8-TBG-cre (KO) were employed and identified (Supporting Fig. S1A). Increased of TG levels were observed in the livers of KO mice relative to control livers (AAV8-TBG-GFP), although no

Author Manuscript

Author Manuscript

Author Manuscript

significant differences were detected in terms of body weight (BW), the ratio of liver weight to BW (LW/BW), hepatic TC and NEFA, serum lipid profiles and  $\beta$ -hydroxybutyrate, or hepatic morphologic changes (Supporting Fig. S1B-F). Since many studies have reported that NAFLD genetic determinants may reinforce the disease phenotype under lifestyle challenges,<sup>(14)</sup> the effects of mGPDH deficiency under HFD challenge were then evaluated. After 12 weeks on a HFD, KO mice exhibited more aggravated hepatic steatosis in comparison to control mice, showing increased LW/BW and liver TG contents. Although hepatic TC and NEFA, serum lipid profiles and  $\beta$ -hydroxybutyrate were still unchanged (Fig. 2A-D), lipid droplets in hepatocytes confirmed by histology and oil red o staining were pronouncedly exacerbated (Fig. 2E), indicating a higher sensitivity of mGPDH KO mice to HFD. Moreover, to address whether the moderate decrease of mGPDH expression observed in HFD mice was sufficient to induce changes in TG accumulation, hemizygous knockout (KO/+) mice were employed. The mGPDH expression was detected in KO/+ mice (Supporting Fig. S2A) and similar results were obtained to mGPDH expression observed after 12 weeks HFD consumption (Supporting Fig. S2B, and Fig. 1A,B). The KO/+ mice showed an intermediate liver TG content and lipid droplet accumulation compared to wild-type and KO mice under HFD conditions (Supporting Fig. S2C-G). Taken together, these results suggest mGPDH deficiency accelerates hepatic TG accumulation and steatosis, which is more pronounced under HFD.

### **mGPDH represses hepatic lipid synthesis**

Author Manuscript

Author Manuscript

TG accumulation is the major contributor to liver steatosis,<sup>(15)</sup> and TG metabolism generally includes lipogenesis, fatty acid oxidation, fatty acid uptake and lipid transport.<sup>(16)</sup> As such, we next sought to determine which aspects of the TG metabolism process were modulated by mGPDH. In LO2 and Huh7 hepatocytes, TG contents and lipid droplets accumulation were enhanced by mGPDH siRNA, while attenuated with mGPDH overexpression, with or without FFA (Fig. 3A,B and Supporting Fig. S3A,B), which was consistent with our in vivo data. mGPDH primarily regulated the expression of lipogenic genes, such as peroxisome proliferator-activated receptor- $\gamma$  (PPAR $\gamma$ ), sterol regulatory element-binding protein-1c (SREBP-1c), acetyl-CoA carboxylase 1 (ACACA), FASN and stearoyl-CoA desaturase 1 (SCD-1), rather than genes related to fatty acid oxidation, fatty acid uptake and lipid transport (Fig. 3C-E).  $\beta$ -hydroxybutyrate (mainly derived from fatty acids oxidation) remained unchanged, which was in accordance with our in vivo results, suggesting that mGPDH did not significantly influence fatty acid oxidation (Supporting Fig. S4A). mGPDH regulation of this lipogenesis pathway was further confirmed in primary hepatocytes isolated from KO mice using <sup>14</sup>C-labeled acetate and gene expression analysis (Fig. 3F,G). Taken together, these findings suggest that mGPDH regulates hepatic TG metabolism by modulating lipogenesis.

### **mGPDH regulates ER-related proteins**

Author Manuscript

Next, we explored the mechanisms underlying the effects of mGPDH. Given that the inflammatory response and insulin signaling are important for liver lipid metabolism,<sup>(17, 18)</sup> these two factors were tested, but no significant changes were observed (Supporting Fig. S4B,C). As a result, we turned to RNA-seq analyses to explore the mechanisms in an unbiasedly manner. Comparison of the mGPDH-overexpression and control groups

identified 1405 RNA species that exhibited statistically significant changes and differential expression (685 upregulated genes and 720 downregulated genes;  $\log_2FC > 1.5$ , Supporting Table S2), and hierarchical clustering of the 30 most highly upregulated and 30 downregulated genes showed distinct patterns for these two groups (Fig. 4A). Biological function analysis for all differentially expressed genes revealed that gene ontology (GO) terms associated with “metabolic process” were notably changed (Fig. 4B and Supporting Table S3). Kyoto Encyclopedia of Genes and Genome (KEGG) analysis showed that mGPDH downregulated the Protein processing in ER, TGF-beta signaling pathway, SNARE interactions in vesicular transport, and other pathways and upregulated Vitamin B6 metabolism, D-Glutamine and D-glutamate metabolism, Spliceosome and other pathways (Fig. 4C and Supporting Table S4). In the mGPDH-downregulated gene set, Protein processing in ER was the most significant term. As the main intracellular site for lipid synthesis, the ER was recently proposed to be crucial for the regulation of hepatic lipid metabolism, and its perturbations (ER stress) reinforced hepatic steatosis.<sup>(19)</sup> Hence, we tested whether mGPDH regulates responses to ER stress. The results showed that mGPDH did regulate the expression of genes involved in ER stress signaling pathways, including activating transcription factor 4 (ATF4), C/EBP homologous protein (CHOP), the spliced form of X-box binding protein 1 (XBP1s) and phosphorylated eukaryotic initiation factor 2 $\alpha$  (p-eIF2 $\alpha$ ) in vitro and in vivo (Fig. 4D,E).

### **mGPDH insufficiency promotes hepatic steatosis by inducing ER stress via the inhibition of Cyp-D ubiquitination**

Next, we addressed the relationship between mGPDH-mediated regulation of lipid metabolism and ER stress. Acute ER stress was induced by the chemical activator TM, which blocks N-linked glycosylation causing ER stress.<sup>(20, 21)</sup> mGPDH KO mice developed more serious ER stress, hepatic steatosis, lipid droplet accumulation, and increased LW/BW and TG content compared with control mice after TM treatment (Fig. 5A-D). These results were consistent with our findings in the HFD-induced chronic ER stress model and suggested that mGPDH deletion enhances susceptibility to both acute and chronic ER stress inducers. Additionally, our results showed that TM did not affect mGPDH RNA and protein levels (Fig. 5A,E), indicating that ER stress has no effect on mGPDH. Moreover, TUDCA, a chemical chaperone that reduces ER stress,<sup>(22)</sup> significantly blunted mGPDH deficiency-induced hepatic steatosis, lipid droplet accumulation, increased LW/BW and TG content and lipogenic gene PPAR $\gamma$  expression in vitro and in vivo (Fig. 5F-K), suggesting mGPDH deletion accelerates TG accumulation and hepatic steatosis via activated ER stress.

Next, we addressed how mGPDH regulated ER stress. Ca<sup>2+</sup> homeostasis has been thought to be vital to lipid-related ER stress in liver,<sup>(19)</sup> and therefore the intercellular Ca<sup>2+</sup> chelator BAPTA-AM was applied. The ER stress induced by mGPDH siRNA was abrogated by BAPTA-AM (Supporting Fig. S5A), indicating mGPDH deficiency-mediated ER stress is Ca<sup>2+</sup>-dependent. Recent studies have shown that multiple mitochondrial proteins cause ER stress by promoting mitochondrial Ca<sup>2+</sup> release.<sup>(23, 24)</sup> mGPDH is located in the inner mitochondrial membrane and may contribute to the regulation of mitochondrial Ca<sup>2+</sup> influx and efflux. We observed that, although the rate of Ca<sup>2+</sup> uptake was unchanged (Supporting Fig. S5B), mitochondrial Ca<sup>2+</sup> release was influenced by mGPDH knockdown or



overexpression (Supporting Fig. S5C). Among the proposed complexes contributing to mitochondrial  $\text{Ca}^{2+}$  release ( $\text{Na}^+/\text{Ca}^{2+}$  exchanger,  $\text{H}^+/\text{Ca}^{2+}$  exchanger and mPTP),<sup>(25)</sup> mPTP persistent opening was reported to lead to ER stress,<sup>(10, 26)</sup> and then we observed whether mGPDH exerted an effect through mPTP. The mPTP inhibitor CsA<sup>(10, 26)</sup> prevented the increase in ER stress markers caused by mGPDH knockdown (Supporting Fig. S5D), indicating mPTP was necessary for mGPDH absence induced ER stress. mPTP mainly includes three constituents, i.e., Cyp-D, voltage-dependent anion channel (VDAC) and adenine nucleotide translocase (ANT-1).<sup>(26)</sup> Although no significant change was observed at the mRNA level for all three constituents (Supporting Fig. S5E), Cyp-D protein levels were regulated by mGPDH (Supporting Fig. S5F). The regulation of mGPDH on Cyp-D protein and its downstream ER stress markers was also observed in LO2 hepatocytes exposed to G3P or in mGPDH KO mice (Supporting Fig. S5G-I). Furthermore, Cyp-D siRNA or shRNA abolished the increased ER stress and lipid biosynthesis induced by mGPDH siRNA or knockout in vitro and in vivo (Supporting Fig. S5J-N), suggesting that the ER stress induced by mGPDH suppression occurred via Cyp-D-controlled mPTP activation. According to a recent report,<sup>(24)</sup> p38 MAPK was implicated downstream of Cyp-D and upstream of ER stress. We, therefore, assessed the impact of mGPDH on the MAP kinases, and the results showed that mGPDH knockout did increase the phosphorylation of p38 MAPK, while ERK and JNK phosphorylation were unchanged (Supporting Fig. S6). In addition, as mGPDH has a known role in mitochondrial bio energetics,<sup>(4, 27)</sup> we observed the impact of mGPDH on ATP and mitochondrial bio energetics. ATP levels showed no significant difference in KO mice compared to control mice (Supporting Fig. S7A), and basal and maximal respiration were also barely changed, although G3P-stimulated respiration was decreased in KO mice (Supporting Fig. S7B).

Then, we explored the mechanism underlying mGPDH regulation of Cyp-D. The Cyp-D protein, but not mRNA level were modulated by mGPDH (Supporting Fig. S5E,F,I), indicating a posttranscriptional mechanism. In addition, Cyp-D protein levels were negatively regulated by mGPDH, and a previous study showed that Cyp-D could be modulated through its degradation by proteasomal pathway,<sup>(28)</sup> we then assessed this pathway. After the addition of the proteasome inhibitor MG-132, the mGPDH overexpression-induced reduction of Cyp-D protein levels was blocked (Supporting Fig. S8A). Furthermore, mGPDH overexpression increased the ubiquitination (Supporting Fig. S8B) and decreased the half-life of the Cyp-D protein (Supporting Fig. S8C), indicating that mGPDH regulated Cyp-D through the ubiquitination-proteasomal degradation pathway.

We also sought clues regarding the mechanism of mGPDH repression during HFD. Altered thyroid hormone levels (T3, T4 and thyroid-stimulating hormone) and thyroid receptor expression ( $\text{TR}\alpha$  and  $\text{TR}\beta$ ) were observed in ob/ob and HFD mice (Supporting Fig. S9A-F). Since it has been reported that thyroid hormone can stimulate mGPDH expression in the liver in a time-dependent manner,<sup>(4, 29, 30)</sup> decreased thyroid hormone and TR levels might contribute to the suppression of mGPDH in the livers of HFD-treated mice. To further explore this possibility, we first examined whether reduced thyroid hormone effects could influence mGPDH expression. Thyroid hormone receptor antagonist (1–850) treatment depressed hepatic mGPDH expression in C57BL/6J mice (Supporting Fig. S9G). Interestingly, the reduction of mGPDH under HFD conditions was not abolished by siRNA

targeting thyroid receptors (TR $\alpha$  or TR $\beta$ ) (Supporting Fig. S9H). These results indicated that although reduced thyroid hormone effects could decrease mGPDH expression, this reduction may not be the main reason underlying the HFD-induced suppression of mGPDH. ROS production was elevated in the liver tissues of HFD-fed mice (Supporting Fig. S10A,B). Moreover, ROS levels showed a decrease in mGPDH KO mice fed with chow diet (Supporting Fig. S10C,D, left), suggesting that reduced mGPDH could suppress ROS to a certain extent. It was reported that mGPDH may represent a risk factor for the overproduction of ROS;<sup>(29, 31, 32)</sup> therefore, these results indicated that downregulation of mGPDH might be an adaptive response to avoid excessive oxidative stress. However, the effects of mGPDH on ROS might be relatively mild compared with the high levels of ROS induced by HFD, which was confirmed by the lack of any significant change in ROS levels in mGPDH KO mice under HFD conditions (Supporting Fig. S10C,D, right).

### Rescue of mGPDH alleviates hepatic steatosis in both HFD- and genetic-induced models

Next, we evaluated the effects of rescuing mGPDH expression to reverse the reduction observed during disease, and a liver-targeted therapeutic gene vector AAV8 was generated.<sup>(33)</sup> Indeed, AAV8-mGPDH treatment led to mGPDH overexpression exclusively in the liver (Supporting Fig. S11A-F). AAV8-mGPDH significantly reduced LW/BW, hepatic TG and lipid droplet accumulation, and steatosis in ob/ob and HFD mice, although no change was observed in serum lipid profiles and  $\beta$ -hydroxybutyric acid (Fig. 6A-C, Fig. 6E-G and Supporting Fig. S12A-D). Interestingly, the liver enzyme activities of ALT and AST were also decreased, indicating liver functions were improved by AAV8-mGPDH (Fig. 6D,H). Moreover, AAV8-mGPDH treatment decreased Cyp-D, ER stress markers and lipogenesis gene expression (Fig. 6I,J), which was consistent with our in vitro mechanism observations. In addition, in agreement with the results obtained with KO mice during HFD, ROS levels were not significantly changed by mGPDH overexpression (Fig. 6K). In sum, these findings indicate that rescue of mGPDH mitigates NAFLD development and may be a promising approach for therapy to treat this pathological condition.

### Discussion

Our observations uncovered an important role of mGPDH deficiency in promoting hepatic steatosis during NAFLD. In our study, both human and mice NAFLD sample analysis provided clinical and basic pathological insights into an association between decreased mGPDH and hepatic steatosis, a correlation that was functionally validated by hepatic mGPDH ablation in vivo and in vitro. Notably, TG accumulation and hepatic steatosis induced by mGPDH deficiency were more serious under HFD condition. This pattern is similar to that reported for some other crucial genes identified in NAFLD, such as transmembrane 6 superfamily member 2 (TM6SF2), which also showed no significant changes under a chow diet, but its loss promotes increased hepatic steatosis after HFD.<sup>(34)</sup> Mounting evidence has suggested that many NAFLD genetic determinants interacting with environmental factors (e.g., sedentary lifestyle, overnutrition and dietary factors) are required to drive NAFLD initiation and progression.<sup>(35, 36)</sup> Our results suggested that mGPDH deficiency might be a new genetic background contributor for NAFLD that accelerates HFD-induced hepatic steatosis. However, the observation time for the chow diet



in our study was relatively short compared to that for HFD, and we could not rule out the possibility that there might be some other developing phenotypes besides increased TG, which would become prominent with an extended observation period under chow diet conditions. In addition, mGPDH primarily regulated TG content, whose accumulation has been proven to be the most notable contribution to hepatic lipid disorder during NAFLD.<sup>(15)</sup> Our results demonstrated that mGPDH mainly influences lipogenesis rather than fatty acid oxidation, fatty acid uptake or lipid transport.

A previous study showed that chronic alcohol consumption increased G3P-driven respiration and protein levels of mGPDH.<sup>(37)</sup> mGPDH is an important pathway that shuttles electrons from cytoplasmic NADH to the mitochondria to regenerate NAD<sup>+</sup> for alcohol metabolism; thus, the upregulation of mGPDH might be an adaptation to chronic alcohol feeding. Our results revealed that mGPDH expression and activity were decreased during NAFLD, suggesting a distinct cellular response and underlying pathogenesis mechanism between NAFLD and AFLD. It has been reported that mGPDH may represent a risk factor for the overproduction of ROS, which would be augmented with an increase in the mGPDH substrate.<sup>(31, 38)</sup> Our results showed that ROS production was induced in the livers of HFD mice. ROS levels were suppressed to a certain extent in mGPDH KO mice fed with normal chow, but were insignificant after HFD challenge. Therefore, HFD-induced downregulation of mGPDH might be an adaptive response to avoid excessive oxidative stress, although this effect seemed to be insufficient to reverse the HFD-induced ROS overproduction. Actually, mGPDH downregulation is a maladaptation because it enhanced ER stress, which led to aggravated NAFLD progression. Additionally, it has been reported that thyroid hormone can stimulate mGPDH expression in the liver in a time-dependent manner.<sup>(4, 29, 30)</sup> However, our results showed that the reduced effects of thyroid hormones might not be the main reason for the suppression of mGPDH during HFD, though it could decrease mGPDH expression under normal chow conditions. Taken together, how HFD suppresses mGPDH warrants further investigation.

We found that mGPDH insufficiency induced ER stress by inhibiting Cyp-D ubiquitination, and this may be an undiscovered mechanism for the initiation of lipid-related chronic ER stress during NAFLD. ER stress has been critically linked to hepatic lipid homeostasis perturbation.<sup>(19, 39, 40)</sup> Our RNA-seq analysis suggested that mGPDH could regulate ER-related proteins, and mice lacking mGPDH were more susceptible to both acute (TM) and chronic (HFD) ER stress inducers. The ER stress inhibitor TUDCA abrogated mGPDH deficiency-induced hepatic steatosis, suggesting that mGPDH effects were exerted via the regulation of ER stress. Furthermore, mGPDH insufficiency induced ER stress mainly through Cyp-D, which is located at the mitochondrial matrix and is considered a key regulator of the mitochondrial Ca<sup>2+</sup> conductance channel mPTP.<sup>(10)</sup> Recent studies have disclosed a regulatory role for Cyp-D/mPTP in ER stress, involving the control of mitochondrial Ca<sup>2+</sup> release.<sup>(24, 28, 41)</sup> Our results provide further evidence for this concept, and indicate that mGPDH might be an upstream regulator of Cyp-D during this process. Our study also suggested that mGPDH regulates Cyp-D degradation via the proteasomal pathway, which is similar to the modulatory mechanism exerted by mitochondrial hematopoietic-substrate-1 associated protein X-1 (HAX-1) on Cyp-D in the heart.<sup>(28)</sup> In addition, Cyp-D regulation of ER stress may be related to ROS and p38 MAPK according to

a recent report.<sup>(24)</sup> While our results showed that mGPDH knockout did not significantly affect ROS levels during HFD, it did increase p38 MAPK, indicating that the induction of p38 MAPK and ER stress by mGPDH deficiency might be independent of ROS; this finding requires more research for clarification. Our KEGG analyses showed that some other pathways were also affected by mGPDH, such as reduced TGF-beta signaling and increased vitamin B6 metabolism. Previous studies have reported several important functions of these pathways in the liver, e.g., TGF-beta is considered a promoter of hepatic fibrosis,<sup>(42)</sup> and vitamin B6 has been referred to as a liver cancer risk reduction agent.<sup>(43)</sup> Therefore, these additional possible effects of mGPDH in hepatic steatosis, fibrosis and cancer, some of which are more likely to occur during the late stages of NAFLD, will be the subject of more investigation. Decreased mitochondrial respiration was also reported to be involved in the development of NAFLD.<sup>(44)</sup> Although mGPDH showed no effect on basal and maximal respiration and ATP levels, its effect on G3P-stimulated respiration is worthy of further investigation to determine its involvement in NAFLD.

Our findings propose mGPDH as a potential therapeutic target for NAFLD. Restoration of mGPDH expression from the reduced levels found in the livers of NAFLD patients and mice significantly attenuated TG accumulation and hepatic steatosis in both HFD- and genetic-induced models. To better observe the effects of mGPDH in the livers, we chose hepatic-specific targeting gene tools in this study, including the hepatocyte-specific promoter-TBG driving cre recombinase and AAV8, which has high hepatic targeting efficiency. Future studies investigating the functional relevance of mGPDH with other tissues and organs are still needed. Additionally, the mouse models adopted in this study are not applicable for studies of hepatic disorders during the later stages, such as NASH, fibrosis or cirrhosis. Thus, as we have mentioned above, the potential effects of mGPDH in the late stages of NAFLD are worthy of further evaluation with corresponding animal models. Another key issue for future studies is to elucidate how mGPDH regulates Cyp-D degradation. Is its enzyme activity required or is this a pleiotropic effect of the protein itself? According to our preliminary results, the addition of G3P decreased Cyp-D and its consequences, indicating that the effect of mGPDH may be related to its enzyme activity, but the possibility of protein effect cannot be ruled out. Moreover, we found that mGPDH influenced the expression of ER stress proteins XBP1, CHOP and ATF4. It was reported that ER stress proteins might also participate in regulating lipogenesis pathway, although their functions remain controversial. For example, XBP1 was shown to activate lipogenesis by inducing SREBP-1c expression<sup>(45)</sup> or by directly binding to the promoters of lipogenic enzymes genes<sup>(46)</sup>. However, this effect of XBP1 is not in line with the observation that IRE (the upstream of XBP1) prevents hepatic steatosis.<sup>(19, 47, 48)</sup> Therefore, it is possible that mGPDH regulates lipogenesis in an ER-dependent manner, but the exact mechanism warrants further investigation.

In summary, our study revealed a role of mGPDH deficiency contributing to hepatic TG accumulation and steatosis. It induced ER stress by inhibiting the degradation of Cyp-D, which might be a new mechanism underlying the initiation of chronic ER stress during NAFLD. Moreover, rescuing hepatic mGPDH might have therapeutic potential for the treatment of this disease.

## Supplementary Material

Refer to Web version on PubMed Central for supplementary material.

## Acknowledgments

### Funding

This work was supported by grants from the National Key R&D Program of China (No. 2017YFC1309602 and No. 2016YFC1101100), the National Natural Science Foundation of China (No. 81471039, No. 81721001, No. 81270893, No. 81401601, No. 81700714 and No. 81600673), NIH (ES027544, DK111436, and CA215591), American Heart Association (30970064), Taishan Scholarship, and the Natural Science Foundation Project of Chongqing (No. cstc2014jcyjqq10006, No. cstc2016jcyjA0518, No. cstc2016jcyjA0093 and No. cstc2017jcyjA1192).

## List of Abbreviations:

<b>AAV</b>	adeno-associated viral
<b>ACACA</b>	acetyl-CoA carboxylase 1
<b>ALT</b>	alanine aminotransferase
<b>ANT-1</b>	adenine nucleotide translocase
<b>AST</b>	aspartate aminotransferase
<b>ATF4</b>	transcription factor 4
<b>BAPTA-AM</b>	1,2-bis (2-aminophenoxy) ethane N,N,N',N'-tetraacetic acid acetoxymethyl ester
<b>BW</b>	body weight
<b>CHOP</b>	C/EBP homologous protein
<b>CHX</b>	cycloheximide
<b>CsA</b>	cyclosporine A
<b>Cyp-D</b>	cyclophilin-D
<b>ER</b>	endoplasmic reticulum
<b>FASN</b>	fatty acid synthase
<b>FFA</b>	free fatty acid
<b>G3P</b>	glycerol-3-phosphate
<b>HAX-1</b>	hematopoietic-substrate-1 associated protein X-1
<b>HDL</b>	high-density lipoprotein cholesterol
<b>LDL</b>	low-density lipoprotein cholesterol
<b>LW</b>	liver weight

<b>mGPDH</b>	mitochondrial glycerol 3-phosphate dehydrogenase
<b>mPTP</b>	mitochondrial permeability transition pore
<b>NAFLD</b>	nonalcoholic fatty liver disease
<b>NEFA</b>	non-esterified fatty acid
<b>OTC</b>	ornithine carbamoyltransferase
<b>PPAR<math>\gamma</math></b>	peroxisome proliferator-activated receptor- $\gamma$
<b>RNA-seq</b>	RNA-sequencing
<b>SCD-1</b>	stearoyl-CoA desaturase 1
<b>SREBP-1c</b>	sterol regulatory element-binding protein-1c
<b>TBG</b>	thyroxine-binding globulin
<b>TC</b>	total cholesterol
<b>TG</b>	triglycerides
<b>TM</b>	tunicamycin
<b>TR</b>	thyroid receptor
<b>TUDCA</b>	tauroursodeoxycholic acid
<b>VDAC</b>	voltage-dependent anion channel
<b>XBP1s</b>	spliced form of X-box binding protein 1

## References

1. Adams LA, Lymp JF, St Sauver J, Sanderson SO, Lindor KD, Feldstein A, et al. The natural history of nonalcoholic fatty liver disease: a population-based cohort study. *Gastroenterology* 2005;129:113–121. [PubMed: 16012941]
2. Anstee QM, Targher G, Day CP. Progression of NAFLD to diabetes mellitus, cardiovascular disease or cirrhosis. *Nat Rev Gastroenterol Hepatol* 2013;10:330–344. [PubMed: 23507799]
3. Eto K, Tsubamoto Y, Terauchi Y, Sugiyama T, Kishimoto T, Takahashi N, et al. Role of NADH shuttle system in glucose-induced activation of mitochondrial metabolism and insulin secretion. *Science* 1999;283:981–985. [PubMed: 9974390]
4. Mracek T, Drahota Z, Houstek J. The function and the role of the mitochondrial glycerol-3-phosphate dehydrogenase in mammalian tissues. *Biochim Biophys Acta* 2013;1827:401–410. [PubMed: 23220394]
5. Thakur S, Daley B, Gaskins K, Vasko VV, Boufraqueh M, Patel D, et al. Metformin Targets Mitochondrial Glycerophosphate Dehydrogenase to Control Rate of Oxidative Phosphorylation and Growth of Thyroid Cancer In Vitro and In Vivo. *Clin Cancer Res* 2018;24:4030–4043. [PubMed: 29691295]
6. DosSantos RA, Alfadda A, Eto K, Kadowaki T, Silva JE. Evidence for a compensated thermogenic defect in transgenic mice lacking the mitochondrial glycerol-3-phosphate dehydrogenase gene. *Endocrinology* 2003;144:5469–5479. [PubMed: 12960027]

7. Kota V, Rai P, Weitzel JM, Middendorff R, Bhande SS, Shivaji S. Role of glycerol-3-phosphate dehydrogenase 2 in mouse sperm capacitation. *Mol Reprod Dev* 2010;77:773–783. [PubMed: 20602492]
8. Madiraju AK, Erion DM, Rahimi Y, Zhang XM, Braddock DT, Albright RA, et al. Metformin suppresses gluconeogenesis by inhibiting mitochondrial glycerophosphate dehydrogenase. *Nature* 2014;510:542–546. [PubMed: 24847880]
9. Liu X, Qu H, Zheng Y, Liao Q, Zhang L, Liao X, et al. Mitochondrial glycerol 3-phosphate dehydrogenase promotes skeletal muscle regeneration. *EMBO Mol Med* 2018;10:9390.
10. Baines CP, Kaiser RA, Purcell NH, Blair NS, Osinska H, Hambleton MA, et al. Loss of cyclophilin D reveals a critical role for mitochondrial permeability transition in cell death. *Nature* 2005;434:658–662. [PubMed: 15800627]
11. Zhao J, Adams A, Roberts B, O'Neil M, Vittal A, Schmitt T, et al. Protein arginine methyl transferase 1- and Jumonji C domain-containing protein 6-dependent arginine methylation regulate hepatocyte nuclear factor 4 alpha expression and hepatocyte proliferation in mice. *Hepatology* 2018;67:1109–1126. [PubMed: 29023917]
12. Ng R, Wu H, Xiao H, Chen X, Willenbring H, Steer CJ, et al. Inhibition of microRNA-24 expression in liver prevents hepatic lipid accumulation and hyperlipidemia. *Hepatology* 2014;60:554–564. [PubMed: 24677249]
13. Wang H, Liu X, Long M, Huang Y, Zhang L, Zhang R, et al. NRF2 activation by antioxidant antidiabetic agents accelerates tumor metastasis. *Sci Transl Med* 2016;8:334ra351.
14. Stender S, Kozlitina J, Nordestgaard BG, Tybjaerg-Hansen A, Hobbs HH, Cohen JC Adiposity amplifies the genetic risk of fatty liver disease conferred by multiple loci. *Nature Genetics* 2017;49:842–847. [PubMed: 28436986]
15. Donnelly KL, Smith CI, Schwarzenberg SJ, Jessurun J, Boldt MD, Parks EJ. Sources of fatty acids stored in liver and secreted via lipoproteins in patients with nonalcoholic fatty liver disease. *J Clin Invest* 2005;115:1343–1351. [PubMed: 15864352]
16. Utzschneider KM, Kahn SE. Review: The role of insulin resistance in nonalcoholic fatty liver disease. *J Clin Endocrinol Metab* 2006;91:4753–4761. [PubMed: 16968800]
17. Henao-Mejia J, Elinav E, Jin C, Hao L, Mehal WZ, Strowig T, et al. Inflammation-mediated dysbiosis regulates progression of NAFLD and obesity. *Nature* 2012;482:179–185. [PubMed: 22297845]
18. Samuel VT, Shulman GI. Integrating Mechanisms for Insulin Resistance: Common Threads and Missing Links. *Cell* 2012;148:852–871. [PubMed: 22385956]
19. Baiceanu A, Mesdom P, Lagouge M, Fougelle F. Endoplasmic reticulum proteostasis in hepatic steatosis. *Nat Rev Endocrinol* 2016;12:710–722. [PubMed: 27516341]
20. Maillou C, Martin J, Sebastian D, Hernandez-Alvarez M, Garcia-Rocha M, Reina O, et al. Circadian- and UPR-dependent control of CPEB4 mediates a translational response to counteract hepatic steatosis under ER stress. *Nat Cell Biol* 2017;19:94–105. [PubMed: 28092655]
21. Hetz C, Bernasconi P, Fisher J, Lee AH, Bassik MC, Antonsson B, et al. Proapoptotic BAX and BAK Modulate the Unfolded Protein Response by a Direct Interaction with IRE1 $\alpha$ . *Science* 2006;312:572–576. [PubMed: 16645094]
22. B P, MF F, TC D, C I, M I, P I, et al. Hepatic p63 regulates steatosis via IKK $\beta$ /ER stress. *Nature Communications* 2017;8:15111.
23. Biczó G, Vegh ET, Shalbueva N, Mareninova OA, Elperin J, Lotshaw E, et al. Mitochondrial Dysfunction, Through Impaired Autophagy, Leads to Endoplasmic Reticulum Stress, Deregulated Lipid Metabolism, and Pancreatitis in Animal Models. *Gastroenterology* 2018;154:689–703. [PubMed: 29074451]
24. Wang X, Du H, Shao S, Bo T, Yu C, Chen W, et al. Cyclophilin D deficiency attenuates mitochondrial perturbation and ameliorates hepatic steatosis. *Hepatology* 2018;68:62–77. [PubMed: 29356058]
25. Stefani DD, Rizzuto R, Pozzan T. Enjoy the Trip: Calcium in Mitochondria Back and Forth. *Annual Review of Biochemistry* 2016;85:161–192.
26. Elrod JW, Molkentin JD. Physiologic functions of cyclophilin D and the mitochondrial permeability transition pore. *Circulation Journal* 2013;77:1111–1122. [PubMed: 23538482]

27. Taleux N, Guigas B, Dubouchaud H, Moreno M, Weitzel JM, Goglia F, et al. High expression of thyroid hormone receptors and mitochondrial glycerol-3-phosphate dehydrogenase in the liver is linked to enhanced fatty acid oxidation in Lou/C, a rat strain resistant to obesity. *J Biol Chem* 2009;284:4308–4316. [PubMed: 19049970]
28. Lam CK, Zhao W, Liu G, Cai W, Gardner G, Adly G, et al. HAX-1 regulates cyclophilin-D levels and mitochondria permeability transition pore in the heart. *Proc Natl Acad Sci U S A* 2015;112:6466–6475.
29. Mracek T, Jesina P, Krivakova P, Bolehovska R, Cervinkova Z, Drahota Z, et al. Time-course of hormonal induction of mitochondrial glycerophosphate dehydrogenase biogenesis in rat liver. *Biochim Biophys Acta* 2005;1726:217–223. [PubMed: 16039782]
30. Dummler K, Muller S, Seitz HJ. Regulation of adenine nucleotide translocase and glycerol 3-phosphate dehydrogenase expression by thyroid hormones in different rat tissues. *Biochem J* 1996;317 (Pt 3):913–918. [PubMed: 8760382]
31. Drahota Z, Rauchova H, Jesina P, Vojtiskova A, Houstek J. Glycerophosphate-dependent peroxide production by brown fat mitochondria from newborn rats. *Gen Physiol Biophys* 2003;22:93–102. [PubMed: 12870704]
32. Mracek T, Pecinova A, Vrbacky M, Drahota Z, Houstek J. High efficiency of ROS production by glycerophosphate dehydrogenase in mammalian mitochondria. *Arch Biochem Biophys* 2009;481:30–36. [PubMed: 18952046]
33. Gao GP, Alvira MR, Wang L, Calcedo R, Johnston J, Wilson JM. Novel adeno-associated viruses from rhesus monkeys as vectors for human gene therapy. *Proc Natl Acad Sci U S A* 2002;99:11854–11859. [PubMed: 12192090]
34. Fan Y, Lu H, Guo Y, Zhu T, Garcia-Barrio MT, Jiang Z, et al. Hepatic Transmembrane 6 Superfamily Member 2 Regulates Cholesterol Metabolism in Mice. *Gastroenterology* 2016;150:1208–1218. [PubMed: 26774178]
35. Anstee QM, Seth D, Day CP. Genetic Factors That Affect Risk of Alcoholic and Nonalcoholic Fatty Liver Disease. *Gastroenterology* 2016;150:1728–1744.e1727. [PubMed: 26873399]
36. Anstee QM, Day CP. The genetics of NAFLD. *Nat Rev Gastroenterol Hepatol* 2013;10:645–655. [PubMed: 24061205]
37. Han D, Johnson HS, Rao MP, Martin G, Sancheti H, Silkwood KH, et al. Mitochondrial remodeling in the liver following chronic alcohol feeding to rats. *Free Radic Biol Med* 2017;102:100–110. [PubMed: 27867097]
38. Orr AL, Quinlan CL, Perevoshchikova IV, Brand MD. A refined analysis of superoxide production by mitochondrial sn-glycerol 3-phosphate dehydrogenase. *J Biol Chem* 2012;287:42921–42935. [PubMed: 23124204]
39. Walter P, Ron D. The unfolded protein response: from stress pathway to homeostatic regulation. *Science* 2011;334:1081–1086. [PubMed: 22116877]
40. Wang S, Kaufman RJ. How does protein misfolding in the endoplasmic reticulum affect lipid metabolism in the liver? *Curr Opin Lipidol* 2014;25:125–132. [PubMed: 24565920]
41. Fujimoto K, Chen Y, Polonsky KS. Targeting cyclophilin D and the mitochondrial permeability transition enhances beta-cell survival and prevents diabetes in Pdx1 deficiency. *Proc Natl Acad Sci U S A* 2010;107:10214–10219. [PubMed: 20479245]
42. Meng XM, Nikolic-Paterson DJ, Lan HY. TGF-beta: the master regulator of fibrosis. *Nat Rev Nephrol* 2016;12:325–338. [PubMed: 27108839]
43. Mocellin S, Briarava M, Pilati P. Vitamin B6 and Cancer Risk: A Field Synopsis and Meta-Analysis. *J Natl Cancer Inst* 2017;109:1–9.
44. Mansouri A, Gattolliat CH, Asselah T. Mitochondrial Dysfunction and Signaling in Chronic Liver Diseases. *Gastroenterology* 2018;155:629–647. [PubMed: 30012333]
45. Ning J, Hong T, Ward A, Pi J, Liu Z, Liu HY, et al. Constitutive role for IRE1alpha-XBP1 signaling pathway in the insulin-mediated hepatic lipogenic program. *Endocrinology* 2011;152:2247–2255. [PubMed: 21447637]
46. Lee AH, Scapa EF, Cohen DE, Glimcher LH. Regulation of hepatic lipogenesis by the transcription factor XBP1. *Science* 2008;320:1492–1496. [PubMed: 18556558]



47. Zhang K, Wang S, Malhotra J, Hassler JR, Back SH, Wang G, et al. The unfolded protein response transducer IRE1alpha prevents ER stress-induced hepatic steatosis. *Embo j* 2011;30:1357–1375. [PubMed: 21407177]
48. Jiang S, Yan C, Fang QC, Shao ML, Zhang YL, Liu Y, et al. Fibroblast growth factor 21 is regulated by the IRE1alpha-XBP1 branch of the unfolded protein response and counteracts endoplasmic reticulum stress-induced hepatic steatosis. *J Biol Chem* 2014;289:29751–29765. [PubMed: 25170079]

Author Manuscript

Author Manuscript

Author Manuscript

Author Manuscript

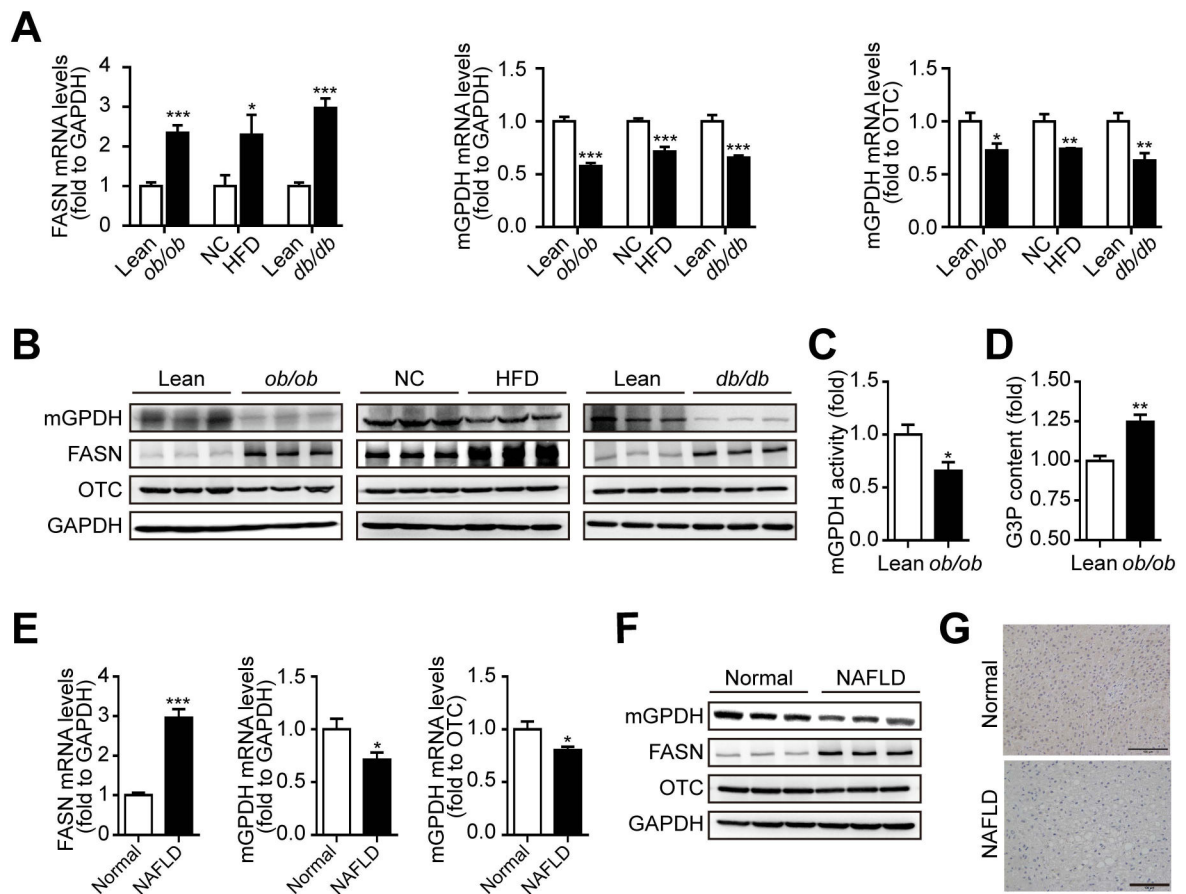


**Figure 1. mGPDH is inhibited in the fatty livers of patients and mice.**

(A and B) The mRNA (A) and protein (B) levels of hepatic mGPDH and FASN in the indicated mice were determined by qRT-PCR and western blot and normalized to ornithine carbamoyltransferase (OTC) and GAPDH. (C and D) The activity of mGPDH (C) and content of the mGPDH substrate G3P (D) were determined by colorimetric assay. (E and F) The mRNA (E) and protein (F) levels of mGPDH and FASN in the livers of NAFLD patients were determined by qRT-PCR and western blot and normalized to OTC and GAPDH. (G) IHC staining of mGPDH on liver sections from patients. Scale bar: 100  $\mu$ m.  $n = 6$  mice or patients per group. Data are presented as the mean  $\pm$  S.E.M. \* $P < 0.05$ , \*\* $P < 0.01$ , \*\*\* $P < 0.001$ .

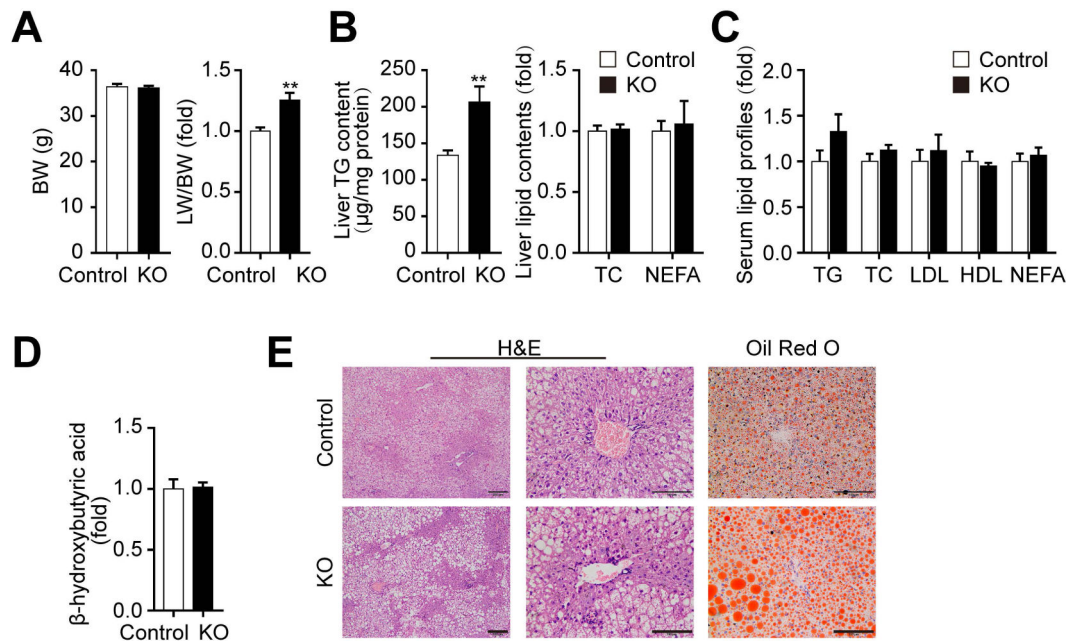


**Figure 2. mGPDH deficiency exacerbates HFD-induced hepatic steatosis.**

Liver-specific mGPDH knockout (KO) and cre-control (control) mice were fed with HFD for 12 weeks, and the (A) body weight (BW) (left) and the ratio of liver weight to BW (LW/BW) (right) were determined. (B) Liver lipid contents (TG, TC and NEFA) were determined enzymatically. (C) The serum lipid profiles (TG, TC, LDL, HDL and NEFA) were tested enzymatically. (D) The serum levels of  $\beta$ -hydroxybutyric acid were determined enzymatically. (E) H&E and oil red o staining of liver sections from KO and control mice. Scale bar: 200 or 100  $\mu$ m.  $n = 6$  mice per group. Data are presented as the mean  $\pm$  S.E.M.

\*\*  $P < 0.01$ .

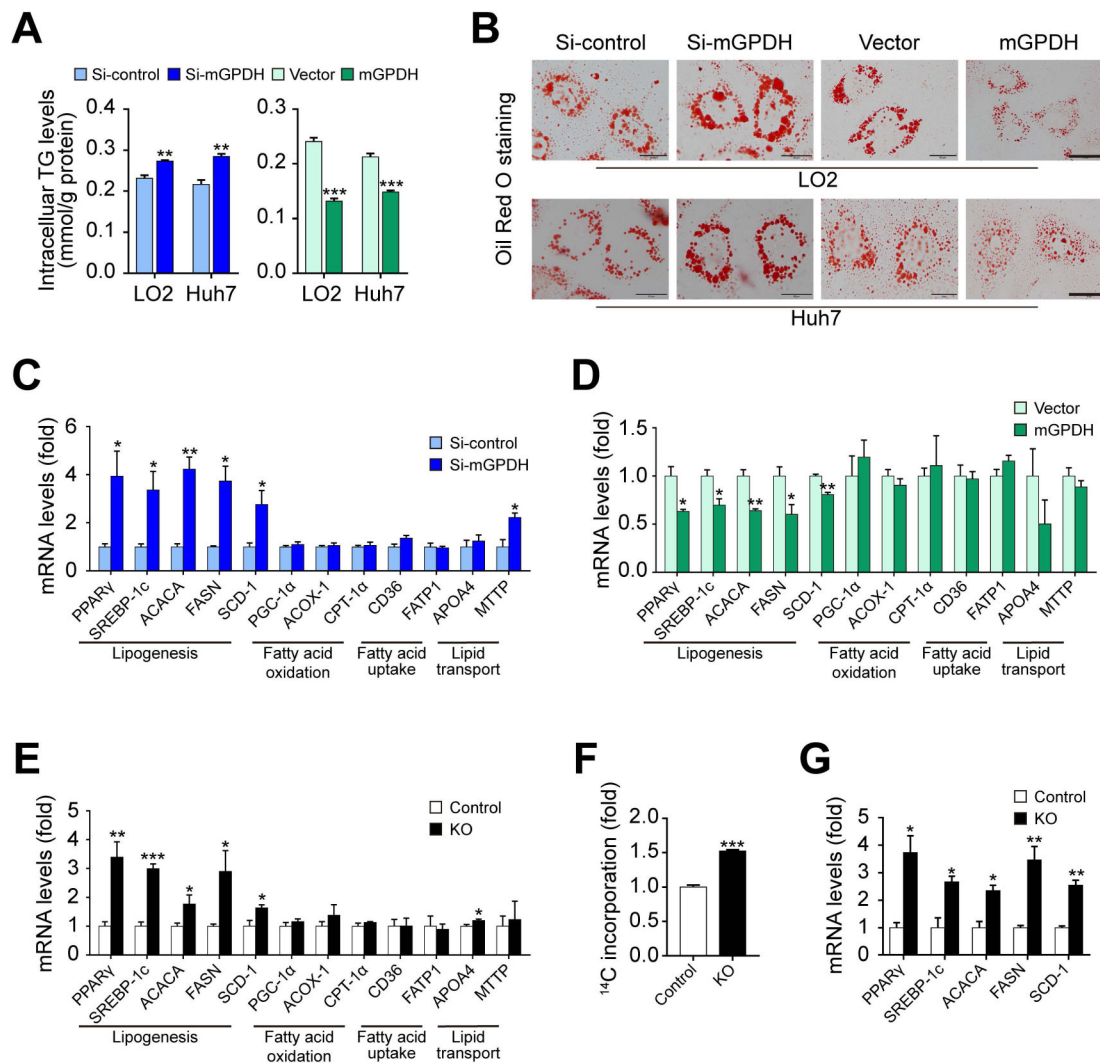


**Figure 3. mGPDH suppresses hepatic lipid synthesis.**

LO2 and Huh7 cells were transfected with siRNA or plasmid for mGPDH inhibition or overexpression and then treated with FFA for 24 h. (A) The TG content was determined enzymatically. (B) Oil red o staining of treated LO2 and Huh7 cells. (C and D) The mRNA levels of genes related to lipid metabolism in mGPDH inhibited (C) or overexpressed (D) LO2 cells were determined by qRT-PCR. (E) The mRNA levels of genes related to lipid metabolism in KO and control mice fed with HFD. (F-G) Primary hepatocytes were isolated from KO and control mice, and de novo lipogenesis (DNL) (F) and mRNA expressions of the DNL pathway (G) were determined. Scale bar: 20  $\mu$ m.  $n = 3$  for A-D, F and G,  $n = 6$  for E. Data are presented as the mean  $\pm$  S.E.M. \* $P < 0.05$ , \*\* $P < 0.01$ , \*\*\* $P < 0.001$ .

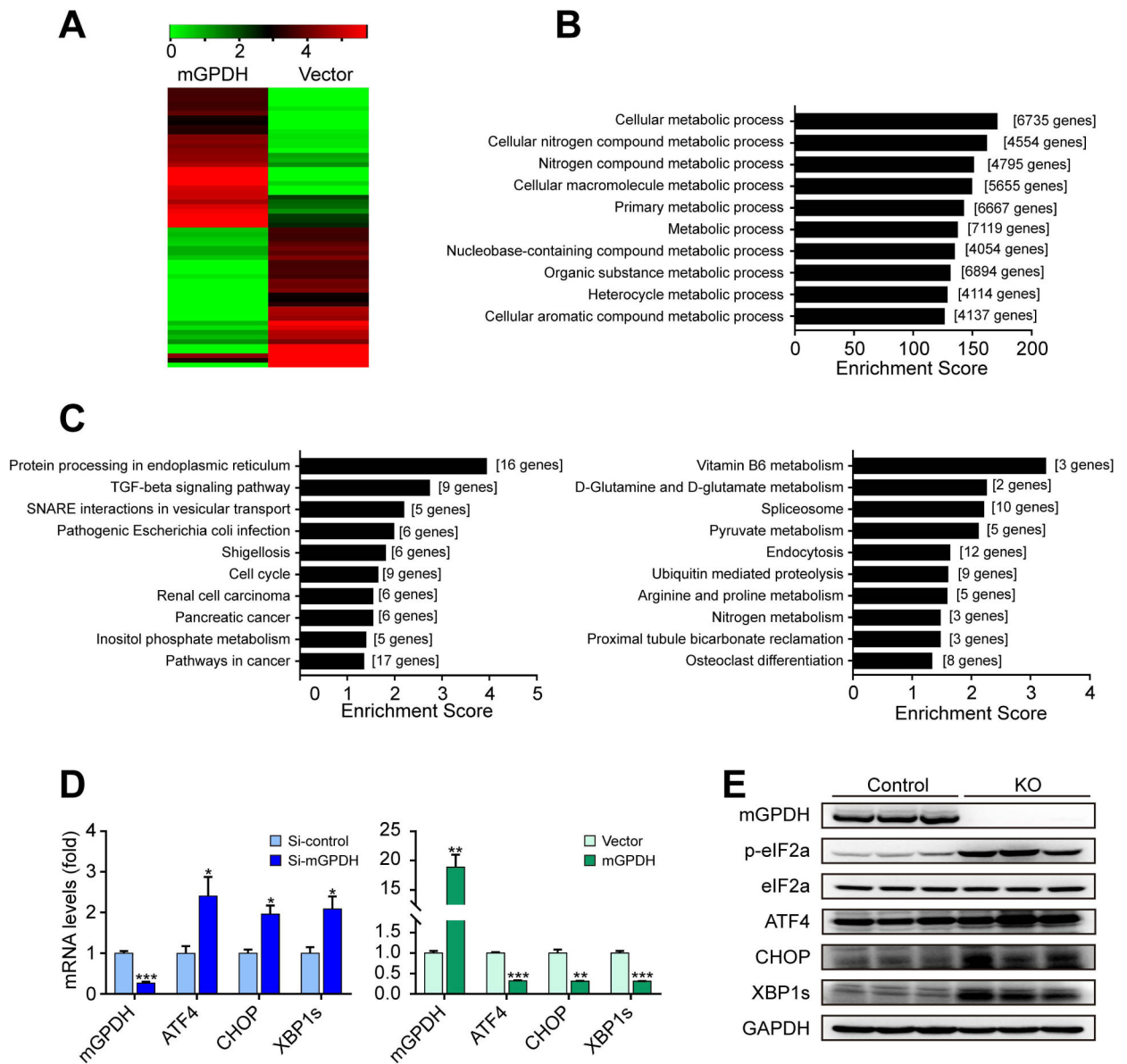


**Figure 4. mGPDH modulates ER-related proteins.**

(A-C) LO2 cells were transfected with pCMV3-N-GFPspark-mGPDH plasmid or vector, and then treated with FFA for 24 h. The heatmap displays the top 30 up- and down-regulated genes (A). GO analysis was conducted with all altered genes, and the ten highest ranking biological process (BP) terms were shown (B). The ten highest ranking terms from KEGG pathway analyses of all significantly down-regulated (left) and up-regulated (right) (change-fold over 1.5) genes were shown (C). (D) LO2 cells were transfected with siRNA or plasmid for mGPDH inhibition or overexpression and then treated with FFA for 24 h, the mRNA levels of mGPDH and ER stress markers (ATF4, CHOP and XBP1s) were detected by qRT-PCR. (E) The hepatic expression of mGPDH and ER stress markers (p-eIF2 $\alpha$ , ATF4, CHOP and XBP1s) in HFD-fed KO and control mice was detected by western blot.  $n = 3$  for A-D,  $n = 6$  mice per group for E. Data are presented as the mean  $\pm$  S.E.M. \* $P < 0.05$ , \*\* $P < 0.01$ , \*\*\* $P < 0.001$ .



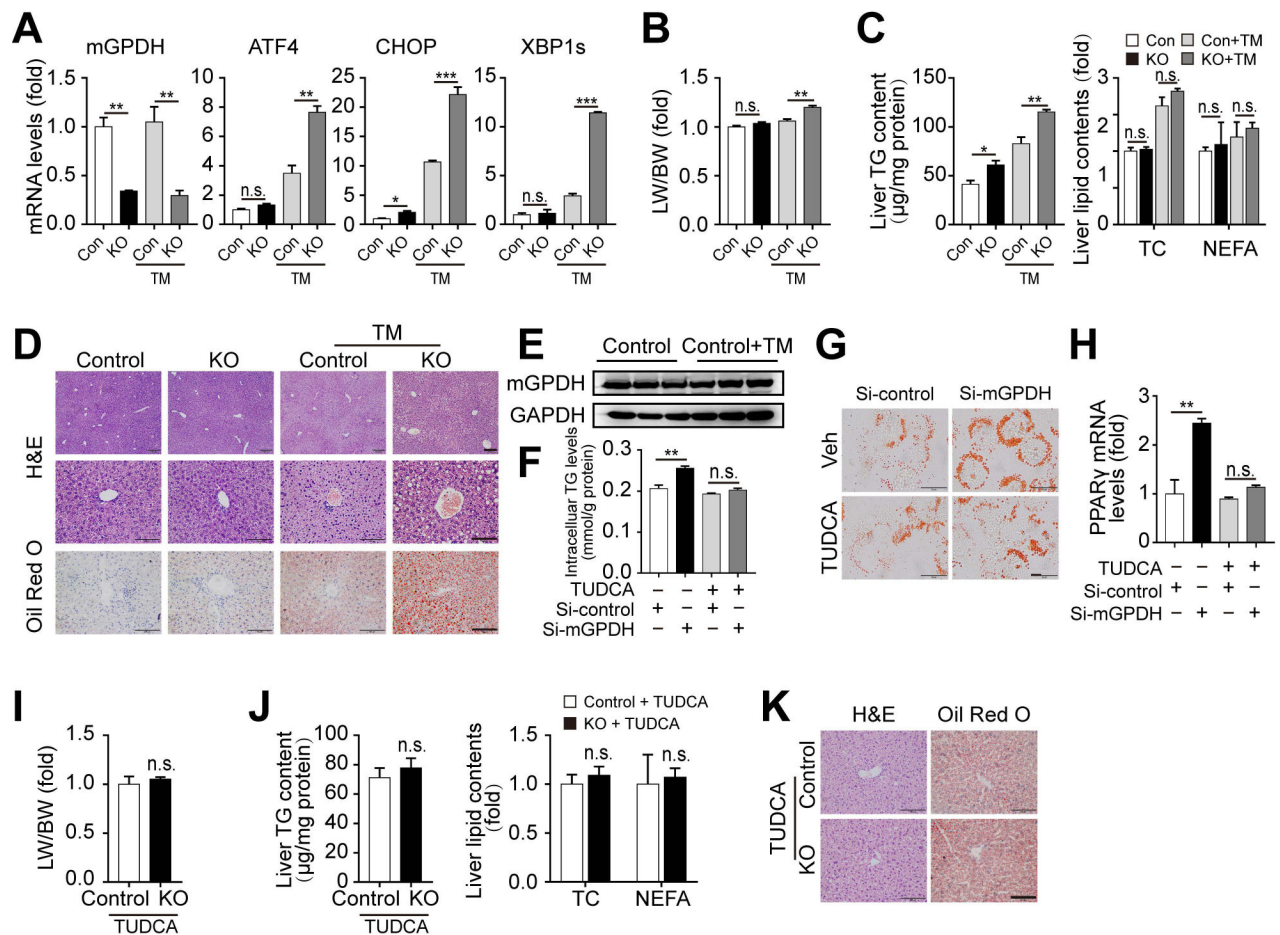


**Figure 5. mGPDH insufficiency promotes hepatic steatosis by inducing ER stress.**

(A-E) KO and control mice were treated with or without TM for 48 h. Hepatic mRNA levels of mGPDH and ER stress markers (A), LW/BW (B) and liver lipid contents (C), and H&E and oil red o staining of liver sections were shown (D). mGPDH protein expression in control mice treated with or without TM (E). (F-H) LO2 cells transfected with mGPDH siRNA were treated with FFA and TUDCA (500  $\mu$ M) for 24 h. TG contents (F), oil red o staining (G) and PPAR $\gamma$  mRNA (H) were determined. (I-K) KO and control mice fed with HFD for 8 weeks were treated with TUDCA (500 mg/kg BW per day per mouse) during the last 2 weeks. LW/BW (I), liver lipid contents (J), and H&E and oil red o staining of liver sections (K) were shown. Scale bars: 200 and 100  $\mu$ m for D, 20  $\mu$ m for G, 100  $\mu$ m for K.  $n = 3$  mice per group for A-E,  $n = 4$  mice per group for I-K,  $n = 3$  for F-H. Data are presented as the mean  $\pm$  S.E.M. \* $P < 0.05$ , \*\* $P < 0.01$ , \*\*\* $P < 0.001$ , n.s., not significant.



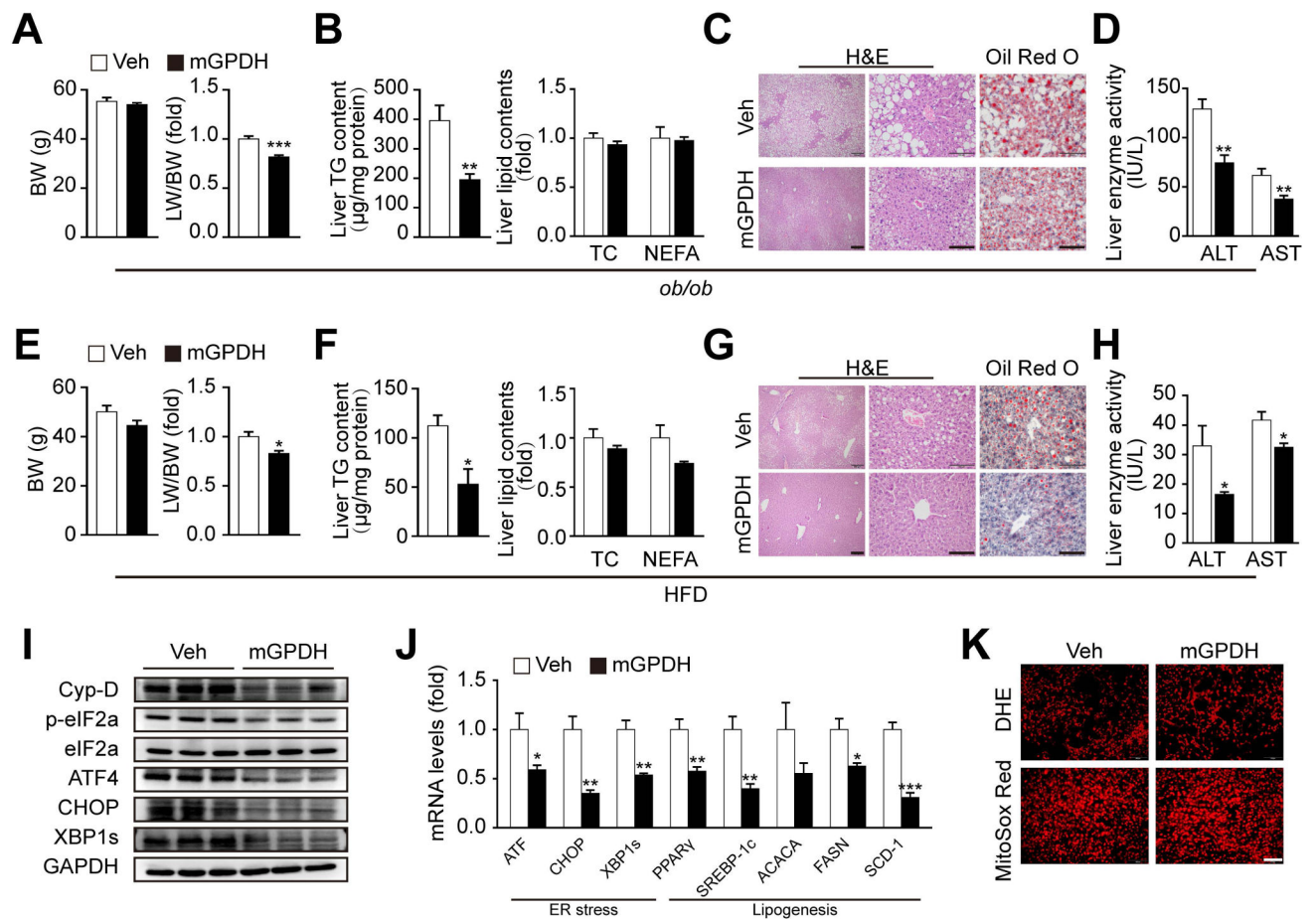


**Figure 6. mGPDH attenuates hepatic steatosis in *ob/ob* and HFD mice.**

(A-D) Eight-week-old *ob/ob* mice were injected with AAV8-mGPDH (mGPDH) or AAV8-GFP (Veh) via the tail vein. BW and LW/BW (A), liver lipid contents (B), H&E and oil red o staining of liver sections (C), and serum levels of liver enzyme activity (ALT and AST) (D) were determined 8 weeks after virus injection. (E-K) C57BL/6J mice were fed with HFD for 12 weeks and at the fifth week of HFD feeding were injected with AAV8-mGPDH or Veh via the tail vein. BW and LW/BW (E), liver lipid contents (F), H&E and oil red o staining of liver sections (G), serum levels of ALT and AST (H), protein levels of Cyp-D and ER stress markers (I), mRNA levels of ER stress markers and lipogenesis genes (J), and ROS levels (K) were determined. Scale bar: 200 or 100  $\mu$ m for C and G, 100  $\mu$ m for K.  $n = 6$  mice per group for A-D,  $n = 5$  mice per group for E-K. Data are presented as the mean  $\pm$  S.E.M. \* $P < 0.05$ , \*\* $P < 0.01$ , \*\*\* $P < 0.001$ .